Available online at www.sciencedirect.com
SCIENCE DIRECT®
Journal of Power Sources 124 (2003) 285–292
JOURNAL OF POWER SOURCES
www.elsevier.com/locate/jpowsour

Research of $Mm(NiMnAlCu)_{4.9}Co_{0.2}$ hydrogen storage alloys prepared by cast and rapidly quenched

Ping Li [a,c,*], Yang-Huang Zhang [a,b], Xin-Lin Wang [a], Yu-Fang Lin [a], Xuan-Hui Qu [c]

[a] *Department of Functional Materials Research, Central Iron and Steel Research Institute, 76 Xuanyuannan Road, Haidian District, Beijing 100081, PR China*
[b] *Department of Material Science and Engineering, Baotou Iron and Steel University of Technology, Baotou 014010, PR China*
[c] *The Power Metallurgy Institute, University of Science and Technology, Beijing 100083, PR China*

Received 3 March 2003; received in revised form 19 May 2003; accepted 21 May 2003

Abstract

The rapidly quenched treatment produced significant effects on the electrochemical characteristics of $Mm(NiMnAlCu)_{4.9}Co_{0.2}$ alloy. It made the activation capability and the discharge capacity decrease, while the cycle stability improved and the degree of the effects increased with increase of the quenching rate. The results of X-ray diffraction analysis showed that the structures of the main phase and secondary phase of $Mm(NiMnAlCu)_{4.9}Co_{0.2}$ alloy are both of the $CaCu_5$ type, but the lattice constants of two structures have a little difference. The amount of the secondary phase in the as-quenched alloy is very little, and rapidly quenched treatment made the structure of the alloy more homogeneous. The lattice constants of the main phase of the as-quenched alloy are larger than that of the as-cast one. Amorphous and crystal co-exist in the alloy with quenching rate of 15 m/s. The Co content was reduced from 10.0 wt.% to 2.8 wt.% through suitable rapidly quenched treatment, and it is not necessary to add other expensive elements in the alloy.

Keywords: Hydrogen storage alloys; Rapidly quenched treatment; Electrochemical characteristics; Microstructure

1. Introduction

In order to further reduce the cost of the AB_5 type rare-earth-based hydrogen storage alloy, several series of AB_5 type hydrogen storage alloys were prepared by adjusting non-stoichiometry and the ratio of Ni, Mn, Al and Co. $Mm(NiMnAl)_{4.9}Co_{0.2}$ and $Mm(NiMnAlCu)_{4.9}Co_{0.2}$ alloys were selected because their discharge capacities, activation performances and high rate discharge capabilities reached applicable levels, but their cycle lives should be improved further [1]. The rapidly quenched technology was applied to improve the cycle life of the $Mm(NiMnAl)_{4.9}Co_{0.2}$ alloy, the results were satisfactory. The cycle life of the alloy with quenching rate of 27 m/s when discharging at 300 mA/g was 243, and it could be activated completely by two cycles when discharging at 60 mA/g with a maximum discharge capacity of 305 mA h/g [2]. The synthetic electrochemical characteristics of the as-quenched alloy $Mm(NiMnAl)_{4.9}Co_{0.2}$ have reached applicable levels, basically, and only the cycle life needs to be improved further. The increased amplitudes of the cycle lives of the alloys with different compositions were different, although the same rapidly quenched technology was applied. The research results of the electrochemical characteristics and the microstructures of the as-quenched alloy $Mm(NiMnAlCu)_{4.9}Co_{0.2}$ will be presented in this paper. The results showed that the effects of the rapidly quenched treatment on the cycle life of the alloy were more significant.

2. Experimental details

2.1. Alloy preparation

The alloy with the composition of $Mm(NiMnAlCu)_{4.9}Co_{0.2}$ was melted in a vacuum induction furnace, in argon atmosphere. After induction melting, the melt was rapidly cooled by pouring into a copper mould cooled by water. Part of the cast alloy was re-melted and quenched by the melt-spinning method, obtaining flakes of the rapidly quenched alloys with quenching rates of 15, 20, 25 and 30 m/s. The quenching rate was expressed by the linear

* Corresponding author. Tel.: +86-10-6218-7570; fax: +86-10-6218-7570.
E-mail address: lpzzg@sina.com (P. Li).

0378-7753/$ – see front matter © 2003 Elsevier B.V. All rights reserved.
doi:10.1016/S0378-7753(03)00628-1

velocity of the copper wheel used for the rapid quenching process. The starting materials were Ni, Co, Mn, Al, and Cu, with purities of over 99.7%, and Mm was Ce-rich mischmetal (24.91 wt.% La, 52.05 wt.% Ce, 5.53 wt.% Pr, 16.93 wt.% Nd) with a purity of 99.42%.

2.2. Electrode preparation and electrochemical measurement

The fractions of both cast and quenched alloys, which were ground mechanically into powder below 250 mesh, were used for the preparation of the electrodes. Electrode pellets with 15 mm in diameter were prepared by mixing 1 g alloy powder with fine nickel powder in a weight ratio of 1:1, together with a small amount of polyvinyl alcohol (PVA) solution as binder, and compressed at a pressure of 3500 kg cm^{-2}. After drying for 4 h, the experimental electrodes were immersed in 6 M KOH solution for at least 1 day, in order to make them fully wet.

Electrochemical measurements were carried out in a tri-electrode open cell with $Ni(OH)_2/Ni(OOH)$ as the positive electrode, Hg/HgO as the reference one, and 6 M KOH solution as electrolyte. Every cycle was overcharged to about 30% with constant current after a 15 min pause. The cut-off potential was −0.500 V. The environment temperature of the measurement was kept at 30 °C. The charge–discharge system was as follows: the activated performance and the maximum discharge capacity were measured through the initial six cycles with a discharge current of 60 mA/g, and then the cycle life and rate discharge capability were measured with a discharge current density of 300 mA/g.

Generally, the cycle life is defined by the number of cycles after which the discharge capacity, reached with constant current charge–discharge at 300 mA h/g, is reduced to 60% of the greatest capacity.

2.3. Microstructure analysis and observation

X-ray diffractometer (type D/max/2400) was used for determining of the phase structures of the alloy samples; the diffraction was performed with Cu Kα and the rays were filtered by graphite. The experimental parameters for determining the phase composition were: 160 mA and 10°/min. The lattice constants were measured by step scanning with experimental parameters of 160 mA, 50 kV and 0.02°/step, and 1/step equivalent to 1.2°/min.

The surface morphologies of the alloy were examined and the micro-zone compositions were analyzed by SEM. The samples of the as-cast alloy were directly polished, and those of the as-quenched alloy were fixed on a grid made of stainless steel when samples were being prepared. The AB_5 type hydrogen storage alloys were etched by 40% fuming nitric acid and 60% alcohol solution and then pulverized by mechanical grinding. The alloy samples thus prepared were dispersed in absolute alcohol for observing the grain morphology with TEM, and for determining, with SAD, whether amorphous phase existed in the alloy samples.

3. Results and discussion

3.1. Electrochemical characteristics of the alloy

3.1.1. The activated capability of the alloy

It was showed in Fig. 1 that the cast alloy could be activated fully through two cycles. The rapidly quenched treatment made the activated number of the alloy increase. The activated numbers of the alloy with quenching rates of 15, 20, 25 and 30 m/s were in the sequence 2, 3, 5 and 7. A lot of literatures [3–5] reported that rapidly quenched treatment decreased the activated capability of the AB_5 type rare-earth-based alloy and AB_2 type Zr-based alloy, and the as-quenched alloy electrode could be activated commonly through five–six cycles. Some of them needed 10 cycles or even more, before the maximum discharge capacity could be obtained. The activated performance of the alloy prepared by gas atomization was poor [6,7]. But Mishima et al. [8] reported that rapidly quenched treatment enhanced the activated performances of the $LaNi_{4.6}Al_{0.4}$ and $LaNi_4Co_{0.6}Al_{0.4}$ hydrogen storage alloys, and Lei et al. [9] reported that the activated capability of the as-quenched alloy $Ml(NiCoMnTi)_5$ was same as that of the as-cast one.

3.1.2. The discharge capacity and the high rate discharge capability of the alloy

Fig. 2 showed that the discharge capacity of the as-quenched alloy was lower than that of the as-cast one, and the high rate discharge capability of the alloy decreased with increase of the quenching rate. The literatures [3–7] reported that rapidly quenched treatment reduced the discharge capacity of the alloy, but [8,9] reported a complete contrary conclusion. The high rate discharge capabilities of the alloys were listed in Table 1. It can be found from Table 1 that the high rate discharge capability of the as-quenched alloy was lower than that of the as-cast alloy.

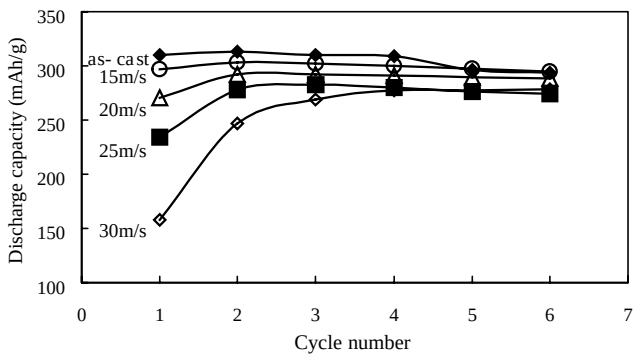

Fig. 1. The activated performances of the as-cast and quenched alloys.

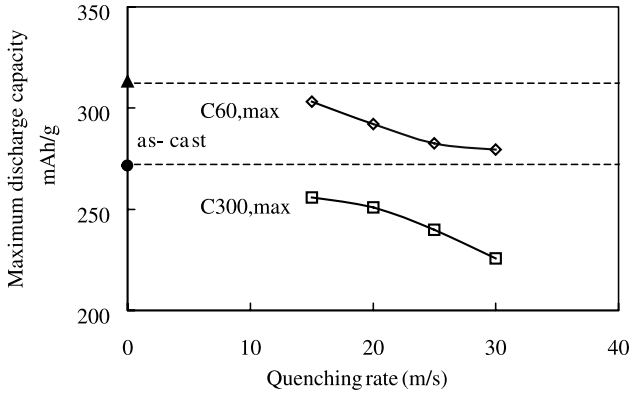

Fig. 2. The maximum discharge capacities of the as-cast and quenched alloys.

Table 1
The high rate discharge capabilities of the as-cast and quenched alloys

	Quenching rate				
	Cast state	15 m/s	20 m/s	25 m/s	30 m/s
High rate discharge capability (%)	86.58	84.37	85.93	84.91	80.75

3.1.3. *The discharge voltage characteristics of the alloys*

In order to compare the characteristics of the discharge voltage plateau, the discharge voltage curves of the alloys with different compositions were put in a figure. The longer and the evener the discharge voltage plateau, the better the discharge characteristics. In addition, the discharge plateau

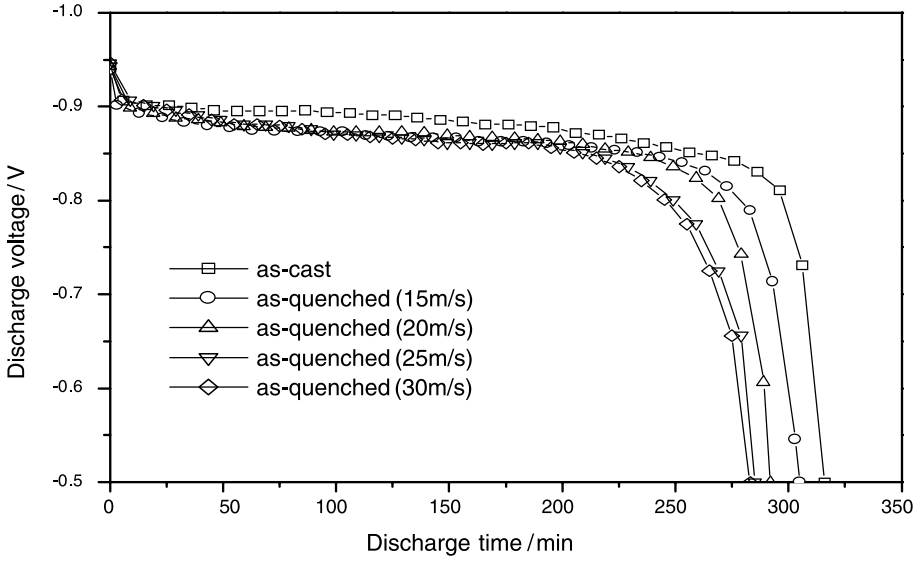

(a) Charge-discharge at 60mA/g

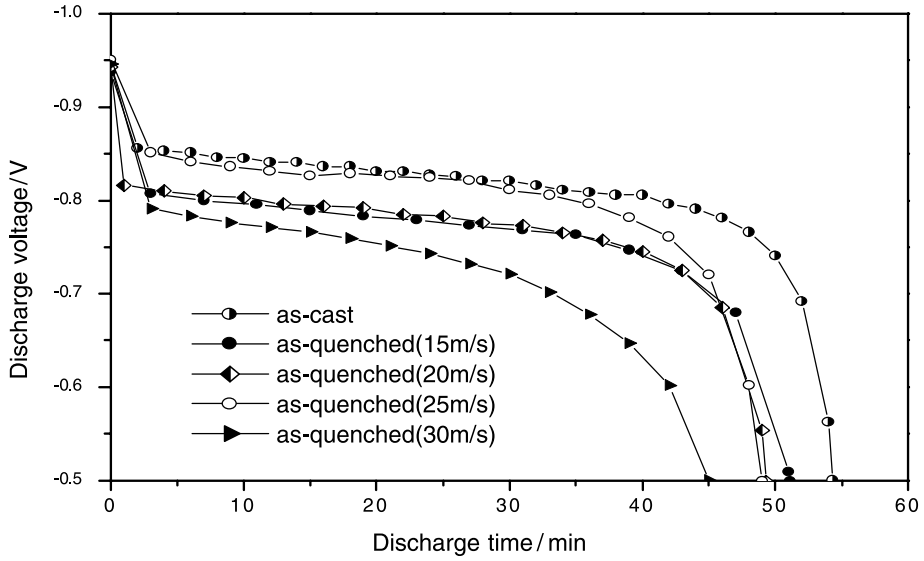

(b) Charge-discharge at 300mA/g

Fig. 3. The discharge voltage characteristics of the as-cast and quenched alloys.

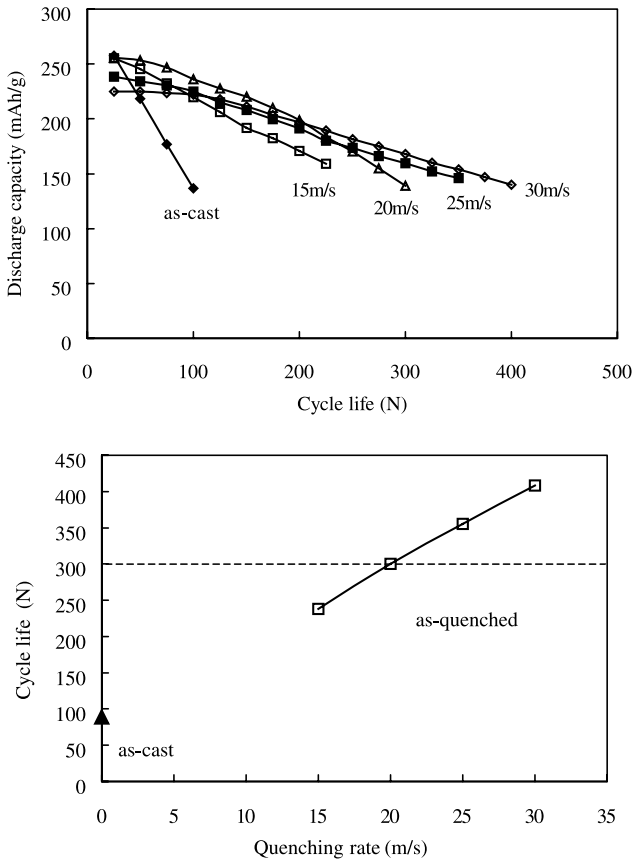

Fig. 4. The cycle lives of the as-cast and quenched alloys.

voltage is an important property. It could be found visibly that the discharge plateau voltage of the as-quenched alloy is lower than that of the as-cast alloy (Fig. 3a); with high rate of discharge, the slope of the discharge voltage plateau of the as-quenched alloy increased obviously (Fig. 3b).

3.1.4. The cycle lives of the alloys

Fig. 4 showed that the cycle life of the as-quenched alloy increased with increase of the quenching rate. The cycle life of the as-quenched alloy with quenching rate of 30 m/s is 408; comparing with the cycle life of the as-cast alloy (86), the increased amplitude was very distinguished. The literatures [3–9] reported the experimental results in which the cycle life could be enhanced significantly by rapidly quenched treatment.

3.2. Determination and observation of microstructure

The analysis of the X-ray diffraction data showed that the structures of the as-cast and quenched alloys with non-stoichiometric composition of $Mm(NiMnAlCu)_{4.9}Co_{0.2}$ are both of $CaCu_5$ type (Fig. 5). It could be seen from Fig. 5 that a high angle peak was split into two or three close peaks, indicated by triangles, and the diffraction diagram of the as-cast alloy had more split peaks than that of the as-quenched one. It should be analyzed whether the separation of Cu Kα double rays lead to this result. Cu Kα ray source consists of Cu $K\alpha_1$ and Cu $K\alpha_2$, their wavelengths being

$$\lambda_{K\alpha_1} = 1.5405\text{Å}$$

$$\lambda_{K\alpha_2} = 1.5443\text{Å}$$

The formula (1) can be obtained according to Bragg formula

$$\theta = \arcsin\left(\frac{n\lambda}{2d}\right) \quad (1)$$

The diffraction angles (2θ), which correspond to several interplanar distances in standard cards of $CaCu_5$ structure, were calculated by formula (1) and taking Cu $K\alpha_1$ and Cu $K\alpha_2$ as diffraction sources, the calculated results were listed in Table 2. It is evident from Table 2 that the low angle peaks produced by Cu $K\alpha_1$ and Cu $K\alpha_2$ are nearly coincident and could not be distinguished, but the high angle peaks produced by Cu $K\alpha_1$ and Cu $K\alpha_2$ could be distinguished obviously, and the peaks produced by Cu $K\alpha_2$ shifted towards high angle. In addition, because the intensity of Cu $K\alpha_1$ ray is twice as large as that of Cu $K\alpha_2$, the intensity of the peak produced by Cu $K\alpha_2$ is half as large as that of the peak produced by Cu $K\alpha_1$. So, we can conclude that the separation of the high angle peak in Fig. 5 was not because of the difference of Cu Kα double ray sources, and also that it was not produced by Cu Kβ because the wavelength difference of Cu Kα and Cu Kβ is about 0.15 Å; this difference can be distinguished at low diffraction angles. So it can be concluded that another phase, with $CaCu_5$ type structure and lattice constants very similar to that of the main phase, existed in the alloy. Because the error produced by the measurement system is smaller in high diffraction angle zone, the slight difference of two phases can be distinguished. There were fewer split peaks in as-quenched alloy. Fig. 6 represented the

Table 2
The split degree of Cu Kα with double rays ($\theta_{\alpha_1} - \theta_{\alpha_2}$)

	(k h l)					
	(1 1 1)	(1 1 2)	(2 2 0)	(4 0 1)	(4 1 1)	(2 2 4)
d (Å)	2.1590	1.5890	1.2742	1.0650	0.9373	0.7945
$2\theta_{\alpha_1}$ (°)	41.80	57.99	74.39	92.47	110.53	151.62
$2\theta_{\alpha_2}$ (°)	41.91	58.15	74.60	92.94	110.93	152.75
$\theta_{\alpha_1} - \theta_{\alpha_2}$ (°)	−0.11	−0.16	−0.21	−0.47	−0.60	−1.12

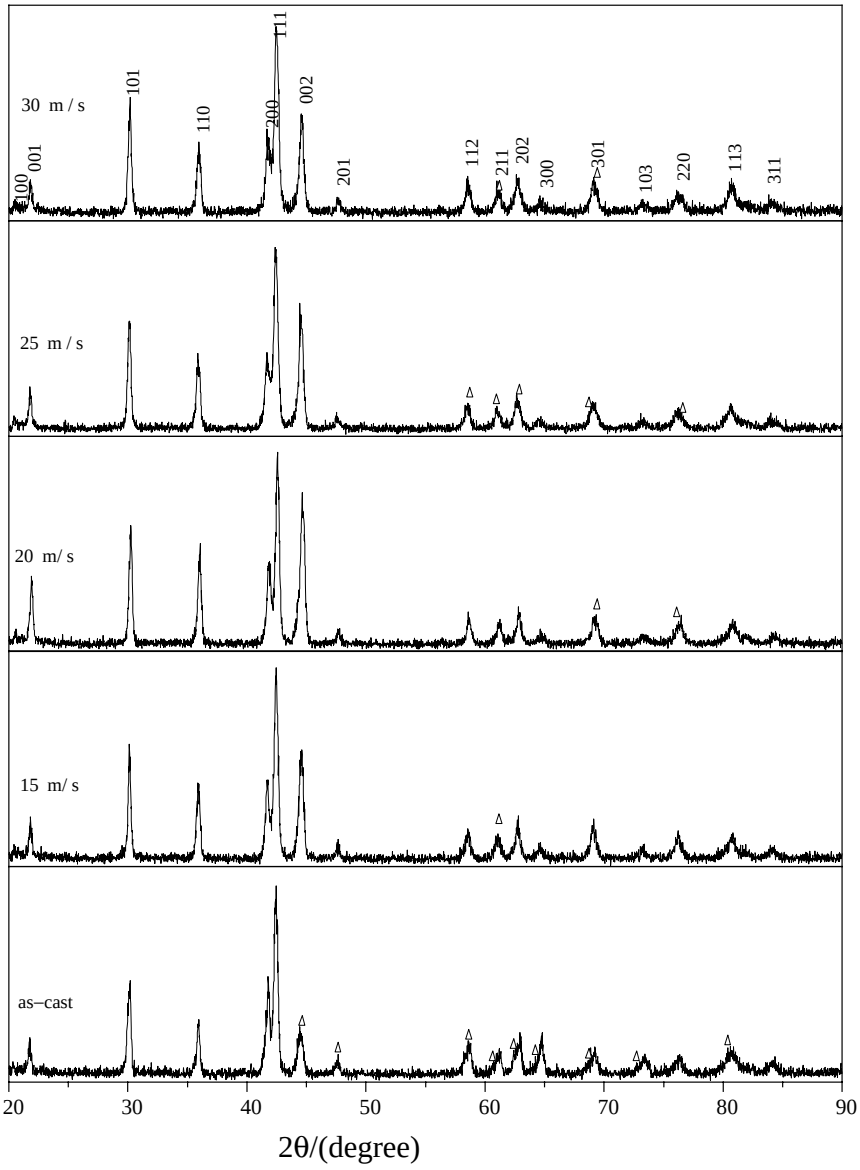

Fig. 5. X-ray diffraction diagrams of the as-cast and quenched alloys (Δ: a high angle peak being split into two or three close peaks).

diffraction diagrams of as-cast and quenched alloys, which were measured by step scanning with diffraction angles from 28° to 46°. It showed that the diffraction peaks of (0 0 1) and (1 1 0) crystal planes of the as-cast alloy also consist of two peaks at low diffraction angles, but the diffraction peaks of the as-quenched alloy were not split in the diffraction angle range from 28° to 46°. The analysis of the X-ray data showed that the structures of the main phase and secondary phase of the alloy were both of $CaCu_5$ type. There was a small amount of the secondary phase in the as-quenched alloy, and the microstructure of the as-quenched alloy was more homogeneous.

Generally, the more homogenous the microstructure, and the larger the high rate discharge capability of the alloy, the better the discharge voltage character. But the high rate discharge capability and the discharge voltage character of the as-quenched alloy $Mm(NiMnAlCu)_{4.9}Co_{0.2}$ were poorer than those of the as-cast alloy; the reason for this result would be researched further.

The lattice constants of the as-cast and quenched alloys were listed in Table 3, which were calculated from the diffraction peaks (1 0 1), (1 1 0), (1 1 1) and (0 0 2) of the main phase of the alloys by a method of least squares. The

Table 3
The lattice parameters of the as-cast and quenched alloys

Quenching rate	Lattice parameters		
	a (Å)	c (Å)	V (Å^3)
Cast state	4.98	4.05	87.0
15 m/s	5.00	4.06	87.9
30 m/s	5.00	4.07	88.1

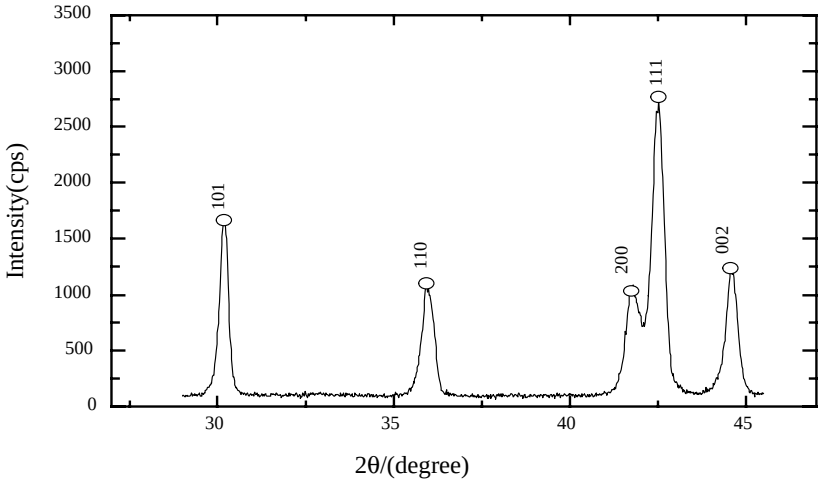

(a) Quenching alloy (15m/s)

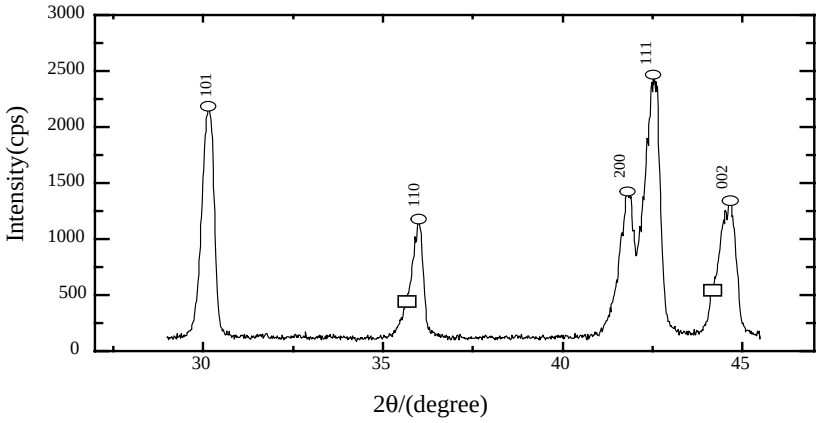

(b) Cast alloy

Fig. 6. X-ray diffraction diagrams of the as-cast and quenched alloys measured by step scanning (□: a diffraction peak being split).

lattice constants of the as-quenched alloy are slightly larger than those of the as-cast alloy. The larger the volume of unit cell, the lower the resolved pressure of hydrogen [10]. This is the main reason why the plateau voltage of the as-quenched alloy is lower than that of the as-cast one.

Although hydrogen storage alloys consist of different elements, and maybe their structures are different, all of hydrogen atoms occupy the interstitial positions of the tetrahedron or octahedron of the alloy lattice. Because the sizes of lattice interstitials (interstitial radius $R_i \approx 0.24$ Å) are smaller than the radius of hydrogen atoms (radius of hydrogen atom $R_h \approx 0.3$ Å), the lattice expansion and distortion are inevitable, and the internal stress is formed when hydrogen atoms enter the interstitial positions. When internal stress is large enough, the lattice would be split, which is pulverization. When the lattice constants increase, the interstitial size of the lattice increases and the volume expansion produced by hydrogen atom entering interstitial decreases, so the pulverization speed of the alloy is reduced. This is the reason why the cycle life of the alloy was enhanced significantly by substituting Al, Co, and Cu for Ni [10]. The larger lattice parameters of the as-quenched alloy $Mm(NiMnAlCu)_{4.9}Co_{0.2}$ are favorable for its cycle life, but the main reason of the as-quenched alloy having excellent cycle stability is because of amorphous phase. The amorphous phase influenced not only the cycle stability of the alloy, but also the discharge capacity and the activation capability of the alloy. A certain amount of amorphous phase existed in the hydrogen storage alloy prepared by rapid quenching, when quenching rate attained a critical value, and the amount of amorphous phase increased with increase of the quenching rate. The amorphous phase produced distinguished influences on the electrochemical characteristics of the alloy. The capacity of $LaNi_5$ amorphous thin film is half as large as that of the crystal alloy. When the state of the alloy transforms from crystal to amorphous, the cycle life of the alloy was enhanced from 10 to 500, the activated number of the alloy was increased from 1∼2 to 10 [11]. The

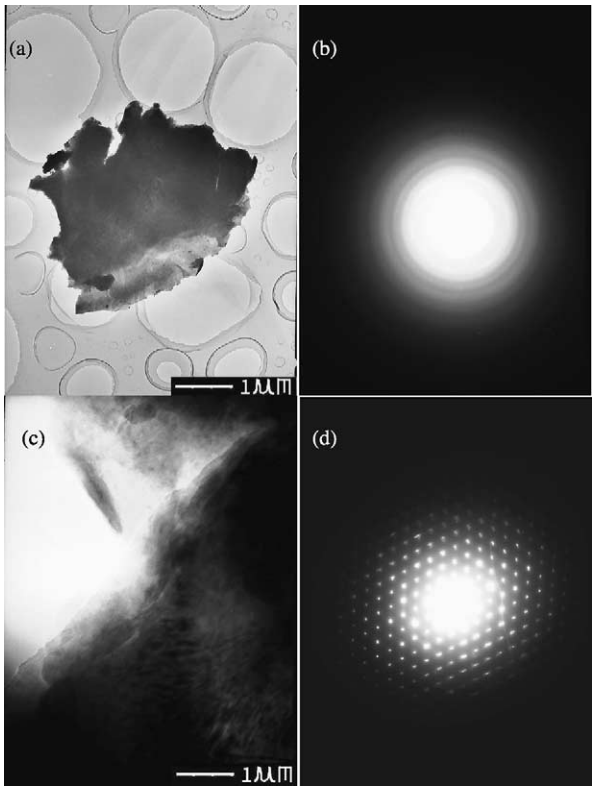

Fig. 7. The microstructure and SAD of the as-quenched alloy (15 m/s) taken by TEM: (a and c) morphologies of the as-quenched alloy; (b and d) SAD of the as-quenched alloy.

quenched alloy had smaller discharge capacity because the amorphous phase, which can absorb little hydrogen, existed in the alloy. The higher the quenching rate, the more is the amorphous phase and the less is the crystal phase; so the discharge capacity of the alloy decreases with the increasing of quenching rate. Hong and co-workers [6] considered that the as-quenched alloy not being activated easily was because the non-fixed form degree of the alloy surface is higher than that of its inside. Li et al. [12] considered that special microstructure of the as-quenched alloy, with co-existence of microcrystal (about 1 μm) and nanocrystal (less than 100 nm) as well as amorphous, played an important role in increasing anti-corrosion and anti-pulverization capabilities of the alloy.

It can be concluded from above-mentioned viewpoints that the amorphous is extremely important for improving electrochemical characteristics of the as-quenched alloy. So, it is very important to determine the critical quenching rate at which the amorphous phase can be formed.

The crystalline and amorphous phases in the quenched alloy, prepared with quenching rate of 15 m/s, were observed and detected by TEM and SAD (Fig. 7). There were some scattered diffraction clouds at the center and several thinner diffraction circles at the periphery of Fig. 7b. This explained that amorphous phase existed in this zone, but it had a crystallized tendency. Fig. 7d showed a diffraction pattern of a complete hexagonal lattice. It could be concluded that the structure of the as-quenched alloy with quenching rate of 15 m/s was co-existing in crystal and amorphous. So, we could assert that amorphous phase existed certainly in the as-quenched alloy $Mm(NiMnAlCu)_{4.9}Co_{0.2}$ when the quenching rate was more than 15 m/s.

The amorphous phase increases with increasing of the quenching rate, but it is very difficult to determine this increase quantitatively. In order to understand the action mechanisms of amorphous and nanocrystal as well as microcrystal on the electrochemical characteristics of the alloy, further investigations are required. The key to the research was to prepare alloy with complete amorphous structure by rapidly quenched technology. We have not yet obtained the complete amorphous hydrogen storage alloy, but the efforts to achieve this are still continuing.

4. Conclusion

1. The rapidly quenched treatment produced significant influences on the electrochemical characteristics of the $Mm(NiMnAlCu)_{4.9}Co_{0.2}$ alloy: it made the activation capability and discharge capacity of the alloy to decrease and the cycle life improved obviously. The activation capability and discharge capacity were reduced and the cycle life was enhanced with the increasing of quenching rate. The discharge voltage characteristic and high rate discharge capability of the as-quenched alloy were slightly lower than those of the as-cast alloy.
2. The structures of the main phase and secondary phase of the alloy $Mm(NiMnAlCu)_{4.9}Co_{0.2}$ are both of $CaCu_5$ type (their lattice constants have a slight difference). The quantity of the secondary phase in the as-quenched alloy is smaller than that of the as-cast alloy, and the structure of the as-quenched alloy is more homogenous.
3. When the quenching rate was 15 m/s, and discharge current densities were 60 and 300 mA/g, respectively, the activated number was 2, the maximum discharge capacities were 303 and 256 mA h/g, the high rate discharge capability was 84.3%, and the cycle life was 238; when quenching rate was 20 m/s, and the discharge current densities were 60 and 300 mA/g, respectively, the high rate discharge capability was 85.93% and the cycle life was 301.
4. The Co content was reduced from 10.0 wt.% to 2.8 wt.% through adjusting rapidly quenched technology, and it is not necessary to add the other expensive elements. The electrochemical characteristics of the alloy could be improved further by using a suitable quenching rate.

Acknowledgements

This work was supported by National Natural Science Foundations of China (50131040 and 50071050).

References

[1] P. Li, X.-L. Wang, Y.-H. Zhang, R. Li, J.-M. Wu, X.-H. Qu, J. Alloys Comp. 353 (2003) 278–282.
[2] P. Li, X.-L. Wang, Y.-H. Zhang, J.-M. Wu, R. Li, X.-H. Qu, J. Alloys Comp. 354 (2003) 310–314.
[3] L.Y. Zhang, J. Alloys Comp. 293-295 (1999) 621–625.
[4] R. Li, J.-M. Wu, X.-L. Wang, J. Alloys Comp. 311 (2000) 40–45.
[5] C.-J. Li, X.-L. Wang, J. Alloys Comp. 274 (1998) 278–283.
[6] Y. Huang, Y. Hui, Z. Hong, J. Alloys Comp. 330–332 (2002) 831–834.
[7] Z. Yu, Y. Lei, Y. Luo, C. Shaoan, Q. Wang, Y. Zhang, J. China Acta Metall. Sin. 32 (8) (1996) 857–861.
[8] R. Mishima, H. Miyamura, T. Sakai, Ni. Kuriyama, H. Ishikawa, I. Uehara, J. Alloys Comp. 192 (1993) 176–178.
[9] Y.Q. Lei, Y. Zhou, Y.C. Luo, X.G. Yang, Q.K. Wang, J. Alloys Comp. 253/254 (1997) 590–594.
[10] J. Zhang, J. Chin. Rare Earths 15 (6) (1994) 54–57.
[11] Y. Li, Y.-T. Cheng, J. Alloys Comp. 223 (1995) 6–10.
[12] C. Li, X. Wang, C. Wang, J. Power Sources 74 (1998) 62–67.